On the investigation of a reliable actuation control method for ohmic RF MEMS switches

Michalis Spasos [1], Rajagopal Nilavalan [2].

(1) Department of Electronics,

Alexander Technological Educational Institute

Sindos, Thessaloniki, GREECE

spasos@el.teithe.gr

+30 2310 013628

(2) Department of Electronic and Computer Engineering

Brunel University

Uxbridge, London, UNITED KINGDOM

rajagopal.nilavalan@brunel.ac.uk

Abstract: Efficient control of RF MEMS switches is a very important issue as it is correlated to main failure mechanisms/modes such as the impact force and bouncing phenomena which degrade their dynamic performance and longevity. This paper presents the control of a specific ohmic RF MEMS switches under three different actuation modes, a tailored pulse optimization method based on Taguchi's technique (voltage mode actuation control), resistive damping (charge mode actuation control) and finally the Hybrid actuation mode, which is a combination of the tailored pulse, the resistive damping and Taguchi's optimization technique. Coventorware simulations indicate that under optimized Tailored pulse and Hybrid actuation modes, the impact velocity is reduced by around 90%, the initial impact force by around 75% and the maximum bouncing displacement during the release phase by around 95%, while the switching speed is increased by around 20% compared with the step pulse control mode. The resistive damping control mode is inappropriate for this type of switch and only partial improvement during the pull-down phase has been achieved.

Finally, a comparison between Hybrid and optimized tailored modes shows that Hybrid actuation mode excels with better switching characteristics and most importantly offers immunity to manufacturing and operation tolerances.

Keywords: RF-MEMS actuation control; tailored pulse; Taguchi optimization; resistive damping.

1. Introduction

State of the art circuitry is necessary to achieve performance and reliability in nowadays radio frequency applications. Switches comprise an important part of many high frequency systems whether they used for power delivery or signal transmission in personal, RADAR or satellite communication systems. Traditional solid state switches are gradually getting substituted by high performance ohmic RF MEMS switches which offer higher isolation and lower insertion loss, lower power dissipation and higher linearity. Their only drawback is mainly that they are usually prone to failure [1], [2].

A reliable ohmic RF-MEMS switch should be capable of switching very fast without settling periods to be necessary due to bouncing phenomena. Additionally, the contact force should be sufficient and constant right after the switch is closed. During the release phase, the switch should return to its null position as fast as possible in order to be ready for the next actuation pulse. In reality, there is always a trade-off between switching speed, settling time and contact force. Fast switching under a voltage step pulse can be achieved by increasing the amplitude of the actuation pulse. Nevertheless, one of the main problems associated with electrostatic actuation under open loop voltage control is the pull-in instability, a saddle node bifurcation phenomenon wherein the cantilever snaps-through to the underneath contact area once its displacement exceeds a certain fraction (typically 1⁄3) of the full gap. Increased cantilever pull-in velocity implies bouncing and settling time is necessary for the switch to perform its best. Moreover, the contact force during the settling period is not constant, reaching undesirable peak values when cantilever touches its corresponding contact area for the first time. That results in unstable contact resistance, power loss and arcing as far as the signal is concerned and induces local hardening, pitting or dislocations in the metal crystal structures of the materials used, reducing the reliability and the longevity of the switch [3].

Although a lot of effort has been put in developing materials capable of maintaining high electrical contact conductance while keeping structural failures low, it still remains one of the major reasons for device failure despite the different control modes (open-loop and closed-loop) that have been introduced by researchers in order to control MEMS electrostatic actuation [4-6].

In terms of the complexity for the driving and sensing electronics, an open-loop approach is superior over a closed-loop control, as it uses only driving circuits. On the other hand, open-loop driving is sensitive to parameter uncertainties. The closed-loop control approach is significantly less sensitive to changes in system parameters and generates oscillation-free response. Nevertheless, closed-loop driving produces relatively slow response and needs complicated hardware.

In terms of application requirements, when an ohmic cantilever type RF-MEMS switch is used, only two signal levels (ON and OFF) are of interest; its switching time usually varies between 2-20μs and the best way to drive it is by using open-loop control. In general there are two main ways for open-loop switching control of RF MEMS switches, using Voltage drive or Charge drive control.

This paper presents the control of a specific ohmic RF MEMS switches under three different actuation modes, a tailored pulse optimization method based on Taguchi's technique (voltage mode actuation control), resistive damping (charge mode actuation control) and finally the Hybrid actuation mode, which is a combination of the tailored pulse, the resistive damping and Taguchi's optimization technique.

The paper is divided into 7 sections. Following the introductory section, which defines the need of efficient control of ohmic RF MEMS switch, **Section 2** presents the "Hammerhead" ohmic RF MEMS switch which is considered in this study. In **Section 3,** the control of the switch via voltage drive (tailored actuation pulse) and the optimization by Taguchi's technique is presented. **Section 4** focuses on the switch's control under charge drive (resistive damping). The control of the switch under Hybrid mode is presented in **Section 5**. In **Section 6** a thorough comparison between the actuation modes is presented, followed by **Section 7** where a comparison between Optimized tailored pulse and Hybrid modes under manufacturing and operational uncertainties is performed. Finally, conclusions and future work are discussed in **Section 8**.

2. The "Hammerhead" ohmic RF MEMS switch

The “Hammerhead” RF-MEMS switch is considered for the case study and is an evaluation of a previously published work [7]. Fig. 1 shows the dimensions of the switch, Fig. 2 the mesh density and the metal layers (magnified 10 times in z axis) and finally Fig. 3 shows the final construction of the switch as extracted from Coventorware.

The simulation results have been extracted under the following environmental conditions: Temperature: 293^{o}K (20^{o}C), Pressure: 730mTorr (1Atm) and Gas type: Nitrogen and a summary of the design parameters of the “Hammerhead” switch is presented in Table 1.

3. Voltage drive control (tailored pulse)

Observing the operation of an ohmic RF-MEMS switch under step pulse implementation at the moment the contact is made, the contact force is very high due to the high impact velocity of the cantilever. The conductance becomes very high but unstable due to the bouncing of the cantilever which follows the first contact, (due to the elastic energy stored in the deformed contact materials and in the cantilever) and it needs time to develop a stable contact force and thereof a stable conductance. This bouncing behavior increases the effective closing time of the switch. Additionally, bouncing affects the opening time (ON to OFF transition) since the cantilever needs time to settle on its null position. That behavior introduces system noise as the distance between cantilever and its corresponding contact point is not constant.

Meanwhile, the contact may get damaged by the large impact force which can be much greater than the high static contact force necessary for low contact resistance. This instantaneous high impact force may induce local hardening or pitting of materials at the contact. Besides, it may facilitate material transfer or contact welding, which is not desirable for a high-reliability switch. All the above increase the adhesive force, which is a function of the maximum contact force and they result contact stiction.

Instead of using a continuous step command to control the electrode, a tailored pulse [8] with different levels of applied voltages and time intervals can be applied, as shown in Fig. 3. The entire operation can be classified in two phases, the “pull down” phase and the “release phase”. The pull down phase mainly refers to the actuation of a contact switch from its original null position to the final contact position.

In the past few years several efforts have been made to tailor the shape of the actuation pulse using either analytical equations on a simplified single-degree-of-freedom (SDOF) model (parallel plate capacitor) on their

own [9-10] or in combination with Simplex optimization algorithms [4], [11]. All these efforts focused on the minimization of the impact force and bouncing during the pull-down phase of the switch but without taking into account damping or adhesion forces. Recently, new publications presented a more accurate solution that includes all the involved parameters [8], [12-14]. Nevertheless, the SDOF model is not considered as an accurate method to describe efficiently a non-linear system like an RF-MEMS switch during its ON–OFF operation. Besides, it is not possible to obtain an analytical expression for damping, with the exception for a linear system with viscous damping. This implies that in all cases mentioned above, the tailored pulse created under analytical expressions implementation, needs to be manually fine-tuned in order to fulfill the requirements for soft landing and bouncing elimination. The main drawback of the above procedure is that there are many parameters that have to be modified in order to reach a good convergence to the targets. Due to the large number of parameters, the nonlinear structure of the device it is very difficult to work it through analytically.

However, the implementation of Taguchi's statistical optimization method [15-16], which is based on Orthogonal Arrays (OA), with Coventorware simulations, shows very good results as it takes into account and other factors like perforation, fringing fields and damping [17].

3.1 Taguchi optimization of the tailored pulse

For an initial estimation of the tailored pulse the analytical method presented by K.-S. Ou et al [8] is followed in order to calculate voltage amplitudes and time intervals. Thus a voltage-pulse train actuation scheme, defined by the attributes listed below and schematically shown in Fig. 4, has been used to improve the dynamic response of the microswitch. These attributes are:

- The amplitude of the actuation voltage *(V_s)*,
- The pull-down actuation time (t_p), which consists of the on time *($t_{p(on)}$)* and the off time *($t_{p(off)}$)*
- The hold-on time ($t_{h(on)}$)
- The release time *(t_r)* which consists of the off time *($t_{r(off)}$)* and the on time *($t_{r(on)}$)*

Making use of this open-loop control technique the bouncing of the switch after the initial contact can be eliminated and the impact force during contact can be minimized while maintaining a fast closing time.

- Initially, a step actuation pulse has been applied to the switch to observe its switching characteristics and verify that there are considerable weaknesses as far as the impact force and the bouncing phenomena are concerned.
- A tailored pulse has been applied next, instead of the single step pulse, based on previously published work [8]. The performance of the switch got better but there was still plenty of room for further improvement.
- Finally, Taguchi's optimization technique has been applied to modify the actuation pulse in order to further improve the behavior of the switch [17].

The objective of Taguchi's algorithm is the minimization of *ff*. According to the nature of the problem two separate optimization procedures have to be realized within two different switching operation phases. The pull-down phase ($ff_{p\text{-}d}$) and the release phase (ff_{r}.)

A. Pull-down phase

The $ff_{p\text{-}d}$ is suitably determined according to the next three conditions.

- Lowest contact time (highest switching speed)
- Lowest contact force (lowest conductance)
- Existence or non existence of a gap (bouncing) after the first contact up to the end of the time interval.

Thus a weighted $ff_{p\text{-}d}$ has been chosen with the form:

Search for time gap between the contact force measurements

If **yes** then $\rightarrow ff_{p-d} = 10^6 \cdot t_{(impact)} + 10^5 \cdot F_{(max)} + 10$

If **no** then $\rightarrow ff_{p-d} = 10^6 \cdot t_{(impact)} + 10^5 \cdot F_{(max)}$

$$ff_{p-d(Log)} = 20Log_{10}(ff_{p-d})$$

where: $t_{(impact)}$ is the time needed for the first contact to occur and $F_{(max)}$ is the maximum impact force measured during the pull-down phase.

B. Release phase

The ff_r is suitably determined according to the difference between maximum and minimum cantilever's displacement, after a predefined time, which includes the pull-down time, the switch-on time and the time that the cantilever needs to reach its zero position after the switch-off.

Thus a weighted ff_r has been chosen with the form:

$$t_{(initial)} > 163\mu sec$$

$$ff_r = 10^4 \cdot (Displacement_{max} - Displacement_{min})$$

$$ff_{r(Log)} = 20Log_{10}(ff_r)$$

where: the $t_{(initial)} > 163\mu sec$ includes the pull-down phase time and the hold-down time (ON) which is terminated at 150μs and an additional 13μs for the switch to reach its null position (OFF), from where the measurements of ± deviation of the cantilever has to be measured. These time intervals have been investigated during the step pulse implementation. The weight-factors (10^4, 10^5, 10^6) are used according to the magnitude (in micron) of the factors and factor 10 indicates the penalty that has to be paid in the case of bouncing during the pull-down phase, otherwise the *ff* could be driven to false results.

Taguchi's method is accurate within a well defined initial area. Thus, taking into account the magnitudes of the tailored actuation pulse of the previous step and considering a ± 20% deviation from these predefined values, the initial levels of the parameters for Taguchi optimization can be created, as shown in Tables 2& 3.

The number of parameters of the actuation pulse which will be calculated through the optimization process are 5 with 3 initial levels each and are considered for the two actuation phases as following:

Pull-down phase (t_P)

A. The magnitude of the pull-down pulse V_p (V)

B. The ON-state of the pulse $t_{p\text{-}on}$ (μs)

C. The fall-time of the pulse $t_{p\text{-}f}$ (μs)

D. The OFF-state of the pulse $t_{p\text{-}off}$ (μs)

E. The rise-time of the pulse $t_{p\text{-}r}$ (μs)

Release phase (t_r)

A. The magnitude of the release pulse V_r (V)

B. The OFF-state of the pulse $t_{r\text{-}off}$ (μs)

C. The rise-time of the pulse $t_{r\text{-}r}$ (μs)

D. The ON-state of the pulse $t_{r\text{-}on}$ (μs)

E. The fall-time of the pulse $t_{r\text{-}f}$ (μs)

For an OA with 5 parameters and 3 levels for each parameter a configuration with at least $n_{rows} = 1 + (k \cdot DOF_m) = 1 + (5 \cdot 2) = 11 rows$ is needed, where DOF_m=*m-1* is the degrees of freedom and in statistical analysis it is equal to the number of the levels of a parameter minus 1.

Taguchi suggests the solution of the $OA_{18}(3^7, 2)$ that can handle up to 7 parameters with 3 levels each and one with 2 levels in an array of 18 rows. For this case 5 columns of the $OA_{18}(3^7,2)$ have been chosen to assign the five parameters in their 3 levels, thus an $OA_{18}(3^5)$ has been created as shown in Table 4. Taking into account the above considerations, the Taguchi's optimization algorithm was implemented in C++ for the actuation pulse.

The optimization procedure graphs, shown in Fig. 5 & 6 present the curves of mean and optimum values for the pull-down and release phase, as they converged through Taguchi process, respectively.

The results for optimum dimensions extracted through Taguchi Optimization method after 20 iterations (less than 1 hour of processing time), for the pull-down and release switching phases of the ohmic RF-MEMS switch are illustrated in Table 5.

Continuing with the analysis, the switch is examined under transient conditions in Coventorware Architect environment. Simulations have been carried out using, initially, a step pulse as an actuation pulse, a tailored pulse and finally the optimized pulse, as described below in Tables 6, 7 and 8, respectively.

Simulating then, the behavior of the switch under the Optimized-Tailored pulse, the results show great improvement with respect to impact velocity (3.6cm/sec instead of 31cm/sec of the step pulse and 5.1cm/sec of

the tailored pulse), which implies true '*soft landing*' of the cantilever, reducing dramatically the impact force (138μN instead of 349μN of the step pulse and 174μN of the tailored pulse), as shown in Fig. 7.

In the pull down phase the bouncing phenomena have been eliminated and the switching speed, is kept high (17μs), around 1.7μs slower than the step pulse (15.3μs), but around 1.5μs faster than the tailored pulse (18.5μs), as shown in Fig.8.

Similar behavior is also observed during the release phase as the ON-OFF switching speed is 13.2μs, around 0.5μs slower than step pulse (12.7μs), but around 1.7μs faster than the tailored pulse (14.9μs). Additionally, bouncing phenomena have practically eliminated (instead of max. deviation of 3.59μm for the step pulse and 0.37μm for the tailored pulse) during the release phase, as in Fig. 9.

A comparison between the results implementing different actuation pulses, are shown in Table 9.

4. Charge drive control (Resistive damping)

Another way to control the impact velocity in order to achieve soft landing and fewer bouncing is the resistive damping. This control method is also referred as charge drive and has been presented for first time by Castaner and Senturia [18]. Under charge control the pull-in phenomenon of the Constant Voltage controlled electrostatic actuators does not exists while, if the current drive is ideal, any position across the gap is stable. The main reason for this behavior is that the applied electrostatic force is always attractive and independent of the remaining gap of the actuator.

Charge drive control using constant current sources is mostly preferred to extend the travel range of electrostatic micro-actuators [19-23]. Nevertheless, there are very few references in the literature as regards charge drive control on RF MEMS. References include, a paper with numerical simulations for a capacitive RF-MEMS by Lee and Goldsmith [24] and another recently published by Blecke et al [25], which presents a learning algorithm for reducing fabrication variability using resistive damping for the pull-down phase. None of these papers presents any details on how to implement resistive damping or any results of such kind of applications. Varehest et al [26], attempted to control the bouncing of a MEMS accelerometer at its resonance frequency using a single resistor.

In case a constant voltage source (V) increases, the electrostatic force is increased due to an increase in the charge (Q).

$$F_e = \frac{QV}{2g}$$

Simultaneously, the increased force decreases the beam height (g), which, in turn, increases the capacitance and its charge. In other words the electrostatic energy (E_k) provided by a constant voltage source (V), is converted to kinetic energy, accelerating the beam [26].

$$E_k = \frac{mV^2}{2}$$

where m=the effective mass of the moving plate.

At $g=2/3g_0$, the increase in the electrostatic force is greater than the increase in the restoring force, resulting in an unstable condition and a collapse of the cantilever beam to the CPW line. This behavior creates a high impact force and bouncing phenomena.

When a voltage source (V_S) with a large series bias resistance is used instead, the behavior of the switch is not the same. The presence of the high bias resistor changes the behavior of the source, to a rather constant capacitor current charge, which mainly depends on the resistor's value. Under these conditions the source behave like a current source and reduces the kinetic energy of the MEMS switch near the point of contact by causing the voltage across the switch (V_C) to drop in case of a rapid change in the capacitance of the electrode area.

$$V_C = V_S\left(1 - e^{-\frac{t}{RC}}\right)$$

The maximum initial charging current of the capacitor which is created under resistive damping between the electrode area and the cantilever during the transition time of the actuation pulse is given by:

$$i_C = C_{el}\frac{dV_C}{dt}$$

where:

C_{el} is the capacitance between the electrode and the cantilever in its initial position.

dV_C is the voltage drop in the capacitor

dt is the rise time of the actuation pulse

The quantification of the bias resistance value for reducing the velocity of the cantilever through the gradual raise of the actuation voltage is calculated through Ohm's law as [27]:

$$R_B = \frac{V_C}{I_C} \qquad \text{or} \qquad R_B = \frac{t_r}{C_{el}}$$

where t_r= the rise time of the actuation pulse

Such a bias resistance cause soft landing with less bouncing phenomena, lower initial impact force but is also introduces additional delay to the switching time.

All the above considerations are valid only for the case that the rise time of the pulse is much smaller than the switching time tr << ts, which means that during the rise time of the pulse the cantilever has not started to move yet and its initial capacitance remains stable.

To eliminate bouncing phenomena, during the release phase of the switch, when the cantilever oscillates in the resonance frequency, the R_BC_{el} product must be equal to the period of the resonance frequency (t_{res}) [26] and the R_b for this case is calculated as:

$$R_B = \frac{t_{res}}{C_{el}}$$

4.1 Implementation of Resistive damping

The "Hammerhead" RF-MEMS switch is considered next for the case study. For the pull-down phase the value of the damping resistance R_B depends on the values of the capacitance, created between the electrode area and the cantilever when the cantilever is in its initial position, and the rise time t_r of the applied pulse, as shown below:

$$R_b C_{el} = t_r = 2\mu m => R_b \approx 17M\Omega$$

where: C_{el} = 118fF, the capacitance created in the electrode area.

Fig. 10 illustrates the characteristics of the switch under step pulse implementation with resistive damping. The results show good switch response during the pull-down phase. Elimination of the bouncing is observed with significant reduction in settling time (35μN from 55μN) and reduction in the initial impact force (169μN from 349μN) with only a small increase in the switching time (18μN from 15μN). In the contrary, very poor response is observed during the release phase. Although the delay in the switching time is 3μm (15μm from 12μm) the effect on the bouncing is very small (3.09μm from 3.59μm). This phenomenon is due to the fact that the movement of the cantilever is governed by different forces.

In the release phase the free move is due to the restoring force and the mechanical resonance frequency of the cantilever and depends only on its elastic properties. Thus, a resistance that can be effective at this phase has to be proportional to the period of the resonance frequency of the cantilever. The resonance frequency of this switch is about 12.3KHz with the period around 80μs and the resulted resistance, calculated for this time, is about R_b = 680MΩ, which unavoidably, is inappropriate for the pull-down phase.

5. Hybrid control mode

A new control method for cantilever type RF-MEMS is presented in this paper for first time and consists of a combination of the two above techniques (Optimized tailored and resistive). The required steps for applying the Hybrid control mode for a given switch is illustrated in the flowchart in Fig.11.

Consider the initial Tailored pulse procedure as in section 3

- Consider the procedure for Resistive damping as in section 4
- Consider the Taguchi optimization procedure as in section 3.1 for a switch controlled by a tailored actuation source in series with the above calculated large bias resistor.

5.1 Implementation of Hybrid control mode

The "Hammerhead" RF-MEMS switch is considered for the case study. The results for optimum dimensions extracted through Taguchi Optimization method after 20 iterations for the pull-down and release switching phases of the ohmic RF-MEMS switch are illustrated in Table 10.

Continuing the analysis, the switch is examined under transient conditions in Coventorware Architect environment. Simulations have been carried out using a voltage source with the characteristics of the optimized pulse, as described in Table 11, in series with a bias resistor of 17MΩ.

Fig. 12 illustrates the characteristics of the Hammerhead switch under Hybrid control mode. The results show good switching characteristics as the impact velocity (1.4cm/sec) has almost eliminated with only a small degradation to switching speed during the pull down phase (19μs) and the release phase (16.5μs). It has to be noted, the gradual increase of the impact force is observed here for the first time with the absence of initial high impact force (84μs).

6. Comparing the actuation modes

A comparison between the four actuation modes (step-pulse, Taguchi optimized tailored pulse, step pulse with resistive damping, and Hybrid) that have been used, is illustrated in Fig. 13. It is obvious that the control of the switch with Optimized tailored pulse mode as well as with Hybrid mode is much better during the release phase as the swing of the cantilever is about 6-7 times smaller.

In Fig. 14 a more detailed view of the pull-down phase is shown, where the actuation of the switch under Optimized tailored pulse, resistive damping or Hybrid mode presents very good behavior, around 17-19μs switching time and almost no bouncing. Under step pulse actuation the switch is faster, roughly 15μs, but with much more initial impact force and with a bounce of about 270nm high.

Comparing the impact force of the switch under the four control modes, the results show good improvement to impact velocity for all three modified actuation modes, 9.4cm/sec for the Resistive, 3.6cm/sec for the Optimized-Tailored and 1.4cm/sec for the Hybrid, instead of 31cm/sec with the step pulse. The Hybrid mode excels all with true *'soft landing'* of the cantilever, dramatically reducing the velocity at the moment the contact is made (by 61% for the Optimized-Tailored, by 85% for the Resistive and by 95% for the Step-pulse) and also the impact force (by 39% for the Optimized-Tailored, by 73% for the Resistive and by 76% for the Step-pulse); with only a small increase in the switching time (by 10% for the Optimized-Tailored, by 4% for the Resistive

and by 19% for the Step-pulse) as shown in Fig. 15. A comparison between the results implementing the four different actuation modes, are shown in Table 12.

7. Optimized tailored pulse and hybrid pulse under manufacturing tolerances

In the real world manufacturing tolerances are very difficult to be avoided. This issue becomes worst in the nano-micro world, especially in MEMS manufacturing and is one of the main reasons of malfunction [11]. Until recently all studies are referred on how to control an RF-MEMS switch under identical conditions and only in 2009 Blecke et al [25] presented a learning algorithm to modify the actuation control in order to face fabrication variability. In this paragraph, the "Hammerhead" switch is considered for fabrication and operational tolerances under the two actuation control modes which appear perfect results in nominal conditions, the Optimized-Tailored and the Hybrid. As fabrication tolerances are considered the thickness of the cantilever in ±5%, the distance between cantilever and electrode in ±5% and the elastic properties of cantilever's material (Au Young Modulus) in three levels 57MP, 78MP and 99MP. As operation tolerance is considered a deviation of ±5% of the calculated actuation voltage amplitude. For reliable results an out of series experiment was designed based on Taguchi's orthogonal design $OA_9 3^4$, which includes four parameters with three levels each, developed in nine series as shown in Table 13.

The results considered under these conditions include the switching time (t_s), the impact force (F_{impact}), the existence of bouncing, the contact force, the magnitude of cantilever's swing during the release phase as well as the failure or not of the switch. The results for the Optimized-Tailored actuation pulse are illustrated in Table 14. In cases 2 and 4 of Table 13, the switch has failed (the cantilever collapsed to electrode). In all other cases the switch is working but presents enough deviation of the nominal values. The results for the Hybrid actuation pulse, as presented in Table 15, are shown a more stable situation without any failure under all the predefined conditions, due to the charge control that introduced through the bias resistor.

An example of how well trimmed is the switch under Hybrid mode, is presented in the Fig. 16 & 17 which represent the conditions of cases 2 and 4 of Table 13. In the same cases the switch under Optimized-Tailored control has been failed. In the case 2 the only change from the nominal conditions is the thickness of the cantilever (5.7μm instead of 6μm). The results for this case under Hybrid mode are almost perfect with an exception of one small bounce during the pull down phase. In case 4 the cantilever's height has been changed

from 3μm to 2.85μm and the actuation voltage from 60V to 63V, creating the worst case for the whole experiment. But even under these circumstances the switch under Hybrid mode has not failed.

8. Conclusion

In this paper all the possible ways to control the actuation of ohmic RF-MEMS switches have been presented and implemented. Apart from the well known control modes, step pulse and tailored pulse, an open loop control procedure based on Taguchi's statistical optimization technique has been presented to improve the operation and, therefore the reliability and longevity of an ohmic RF-MEMS switch. This technique allows exact calculation of the time intervals and voltage magnitudes required by the actuation pulse train to reduce the impact velocity by 41.6%, the impact force by 20%, the maximum bouncing during the release phase by 70% and the switching time by 8% compared with the calculated tailored pulse under analytical method.

Following that, a quantification of the existing method of resistive damping (charge control) has been presented, allowing the exact calculation of the Bias resistor in order to reduce the impact force hence during the pull-down phase. Nevertheless, resisting damping is inappropriate for switches with low resonance frequency as it is not possible to reduce the bouncing swing during the release phase.

Finally, a new technique, the Hybrid control mode, has been presented. This new open loop technique is based on the combination of the two previously mentioned methods (Taguchi's optimized tailored pulse and resistive damping). The simulation process has been carried out in the Architect module of Coventorware® and presents true 'soft landing' through reducing the impact velocity by 61%, the initial impact force by 39% and increasing only the switching time by 10% compared to the optimized tailored pulse mode. Moreover the Hybrid control mode ensures among others, immunity to manufacturing and operation uncertainties with good switching characteristics that have been achieved under Optimized tailored pulse. . Hybrid control method is valid only with relatively slow switches with switching time ($t_s > 10\mu s$) for efficient tailored pulse implementation.

This research work is still ongoing aiming at the fabrication of the switch in order to verify the simulation results and the validity of the Hybrid method. Another future task is the efficient control of more stiff devices and the extraction of a general rule that can be applied to any ohmic RF MEMS switch.

References

1. G. Rebeiz, RF MEMS: Theory, Design, and Technology, John Wiley & Sons, 2003.
2. J. McKillop, RF-MEMS: Ready for Prime Time, Microwave Journal, February 2007.
3. H. Newman, et al, Lifetime measurements on a high-reliability RF-MEMS contact switch, IEEE, Microwave and wireless component letters, 18 (2008) 100-102.
4. H. Sumali, et al, Waveform design for pulse-and-hold electrostatic actuation in MEMS, Elsevier, J. of Actuators and Sensors, (2006) 213-220
5. B. Borovic, et al, Open-loop versus closed-loop control of MEMS devices: choices and issues, IOP, J. of Micromechanics and Microengineering, 6 (2005) 1917–1924.
6. L. Castaner, Drive methods for electrostatic MEMS switches, UIC seminar, Barcelona, Spain, 2005.
7. M. Spasos, et al, An easy to control all-metal in-line-series ohmic RF-MEMS switch, Springer, J. of Analog Integrated Circuits and Signal Processing, 65 (2010)
8. K. Ou, et al, A command shaping approach to enhance the dynamic performance and longevity of contact switches, Elsevier, J. of Mechatronics, (2008) 375-389.
9. D. Czaplewski, et al, A Soft-landing waveform for actuation of a single-pole single-throw ohmic RF-MEMS switch, IEEE, J. of Microelectromechanical systems, 15 (2006) 1586-1594.
10. J. Massad, et al, Modeling, simulation, and testing of the mechanical Dynamics of an RF-MEMS switch, International conference on MEMS, NANO and smart systems (ICMENS'05), 2005.
11. M. Allen, R. Field, and J. Massad, Modeling and input optimization under uncertainty for a collection of RF-MEMS devices, Chicago, ASME International mechanical engineering congress and exposition, 2006.
12. M. F. Daqaq, et al, Input-shaping control of nonlinear MEMS, Springer, J. of Nonlinear Dynamics, 54 (2008) 167-179.
13. C. Do, et al, Dual-pulse control to eliminate bouncing of ohmic RF-MEMS switch. Cork, Ireland, In Proceedings of ISSC, 2010.
14. Z. Guo, N. McGruer, and Adams, Modeling simulation and measurement of the dynamic performance of an ohmic contact electrostatically actuated RF-MEMS switch, IOP, J. of Micromechanics and Microengineering, (2007) 1899-1909.
15. G. Taguchi and Y. Yokoyama, Taguchi methods: Design of experiments, Quality engineering, Vol. 4, Amer Supplier Institute, 1993.

16. G. Taguchi, S. Chowdhury and Y. Wu, Taguchi's quality engineering handbook, Wiley-Interscience, 2004.

17. M. Spasos, et al, RF-MEMS switch actuation pulse optimization using Taguchi's method, Springer, J. of Microsystems Technologies, 17 (2011) 1351-1359.

18. L. Castaner, S. Senturia, Speed-energy optimization of electrostatic actuators based on pull-in, IEEE, J. of Microelectromechanical Systems, 8 (1999) 290-298.

19. S. Senturia, Microsystem design, Kluwer Academic Publishers, N.Y., USA, 2002.

20. L. Castaner, et al, Analysis of the extended operation range of electrostatic actuators by current-pulse drive, Elsevier, J. of Sensors and Actuators, 90 (2001) 181-190.

21. R. Nadal-Guardia, et al, Current drive methods to extend the range of travel of electrostatic microactuators beyond the voltage pull-in point, J. of Microelectromechanical Systems, 11 (2002) 255-263.

22. V. Jimenez, et al, Transient dynamics of a MEMS variable capacitor driven with a Dickson charge pump, Elsevier, J. of Sensors and Actuators, 128 (2006) 89-97

23. J. Pons-Nin, et al, Voltage and pull-in time in current drive of electrostatic actuators, IEEE, J. of Microelectromechanical Systems 11 (2002) 196-205..

24. J. Lee and C. Goldsmith, Numerical simulations of novel constant-charge biasing method for capacitive RF-MEMS switch, San Francisco, CA, In Proceedings of NanoTech conference, 2003.

25. J. Blecke, et al, A simple learning control to eliminate RF-MEMS switch bounce, IEEE, J. of Microelectromechanical Systems, 18 (2009) 458-465.

26. M. Varehest, et al, Resistive damping of pulse-sensed capacitive position sensors, TRANSDUCERS '97, International conference on Solid-state Sensors and Actuators, IEEE, 1997.

27. M. Spasos, et al, Improving controllability in RF-MEMS switches using resistive damping, Athens, Greece, EUMA, MEMSWAVE, 2011

Figure captions

Fig. 1. Dimensions of the “Hammerhead” RF-MEMS switch

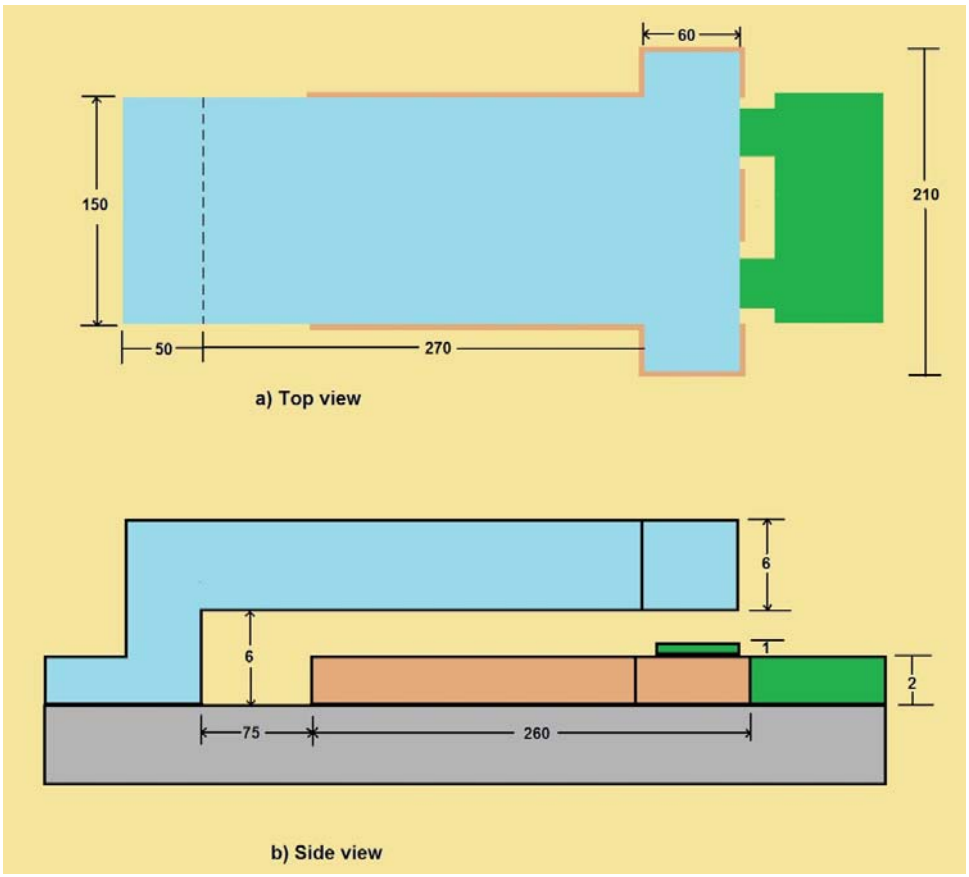

Fig. 2. The meshed design

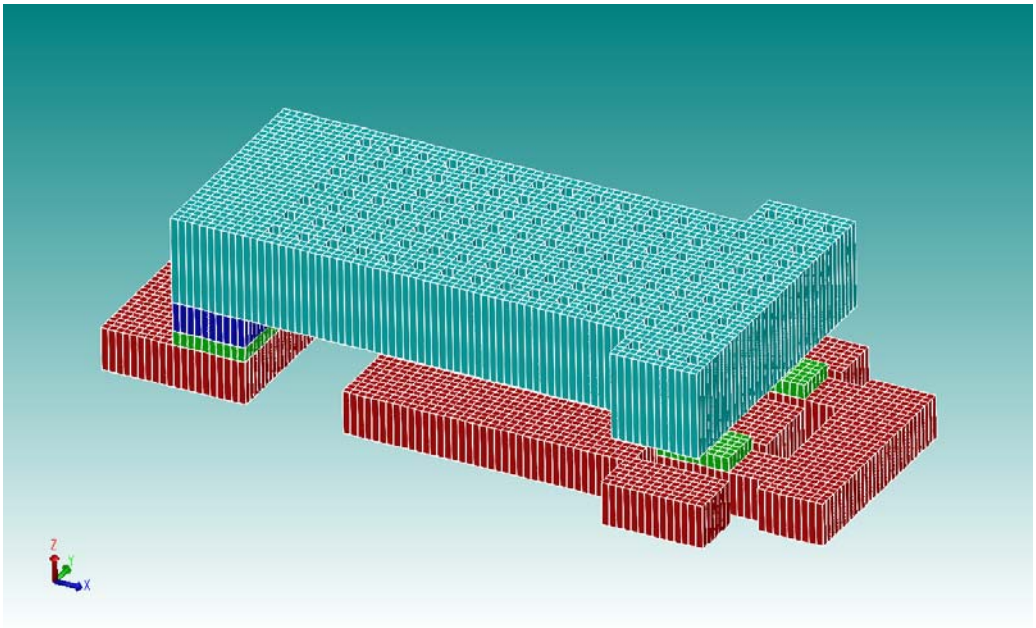

Fig. 3. The “Hammerhead” ohmic RF MEMS Switch as extracted from Coventorware

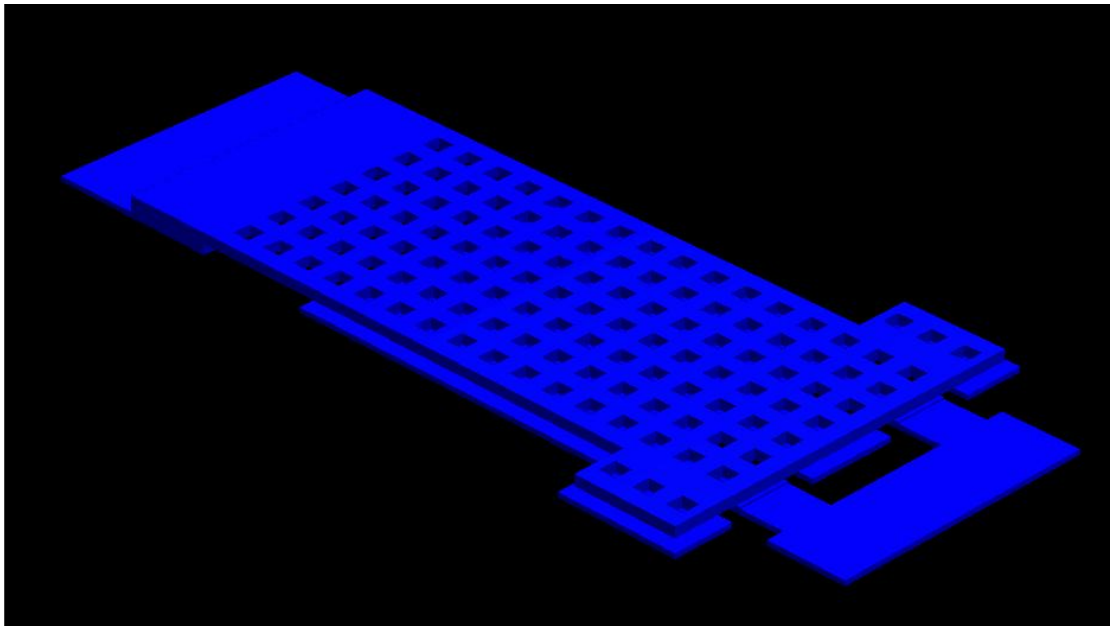

Fig. 4. The phases of the tailored actuation pulse

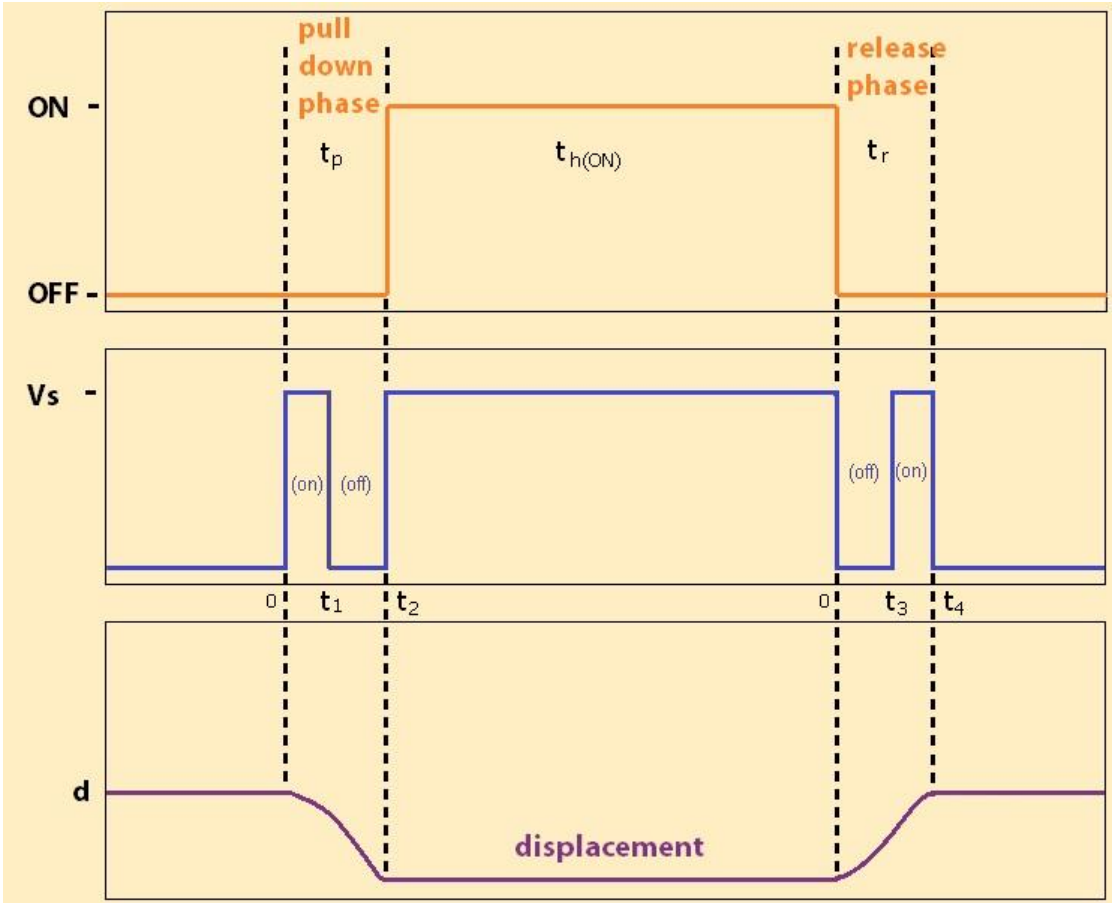

Fig. 5. Optimization procedure graph for the Pull-down phase of the switch

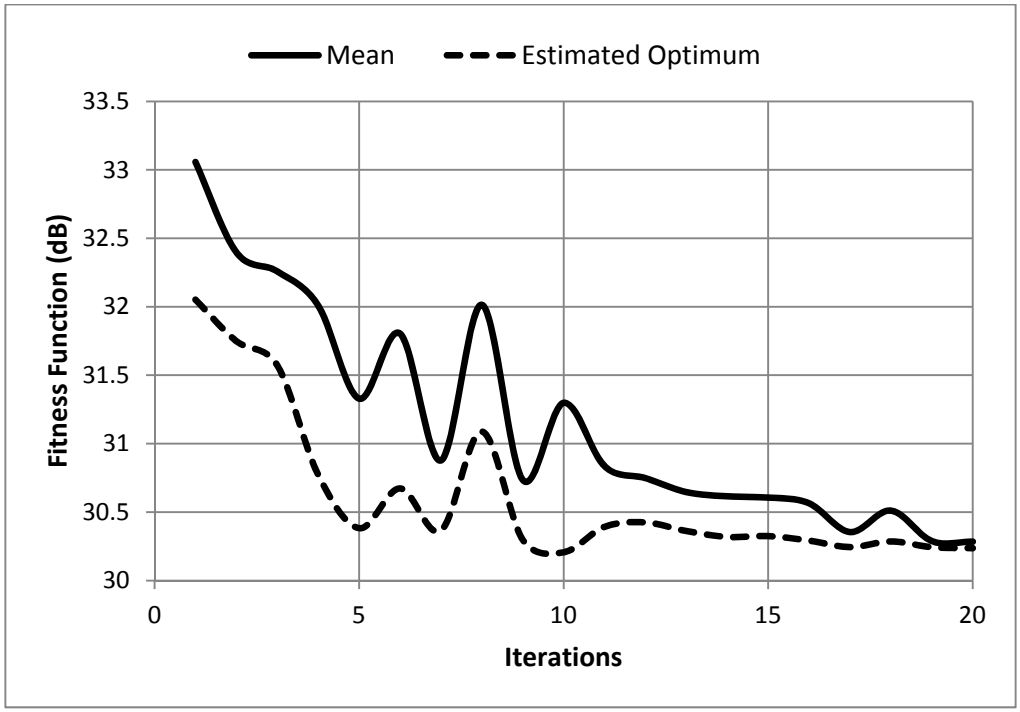

Fig. 6. Optimization procedure graph for the Release phase of the switch

Fig. 7. Comparison of the contact forces

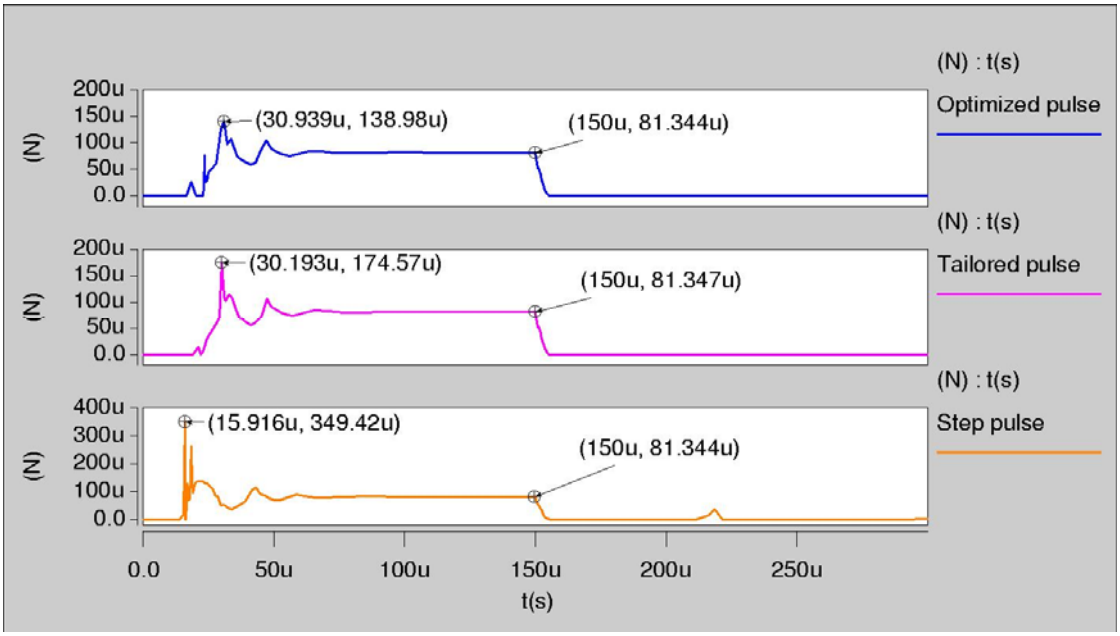

Fig. 8. Comparison of the switching behavior during the pull down phase

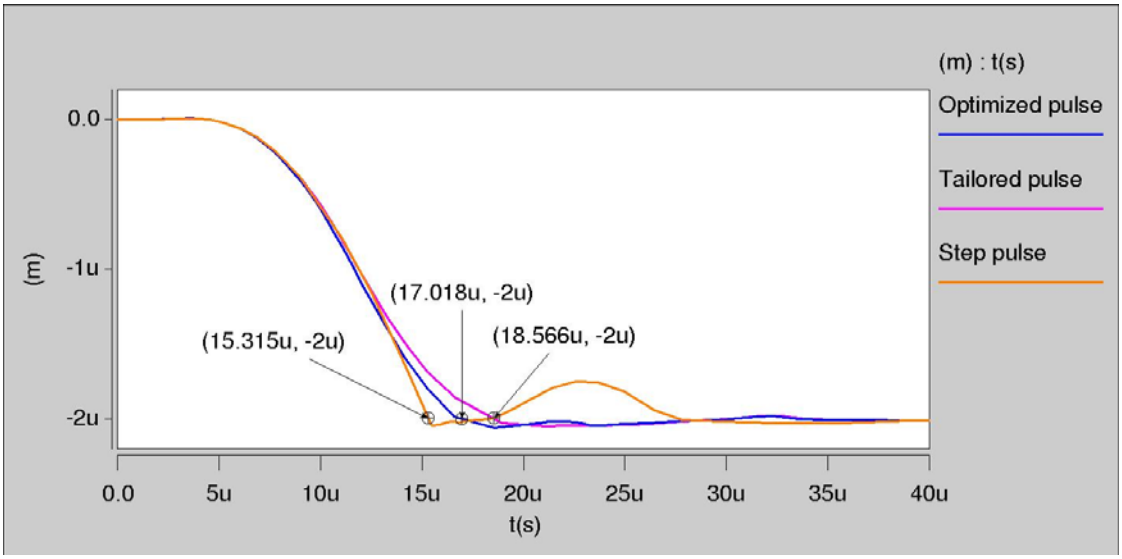

Fig. 9. Comparison of the switching behavior during the release phase

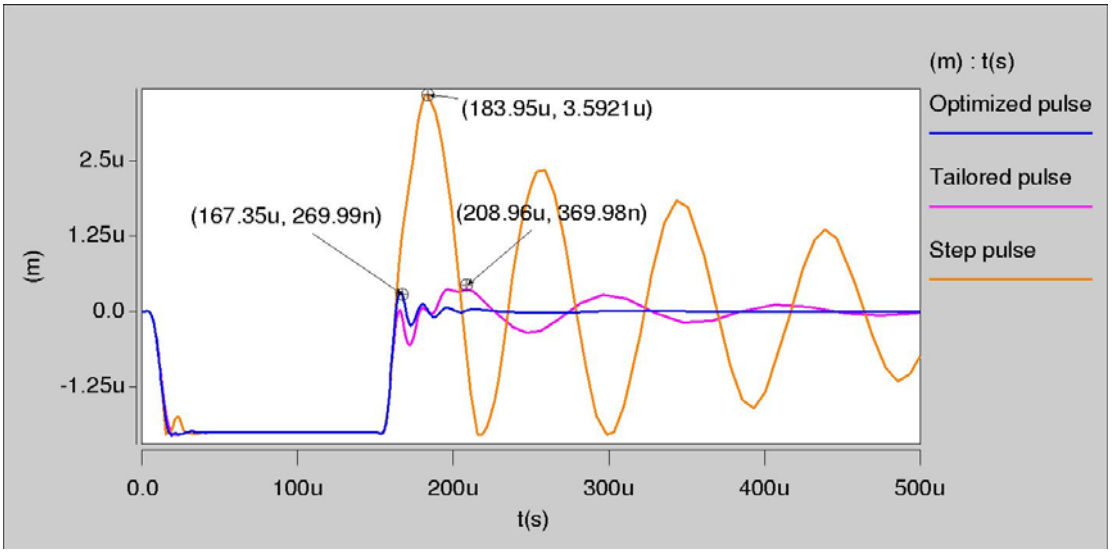

Fig. 10. Characteristics of the switch under resistive damping

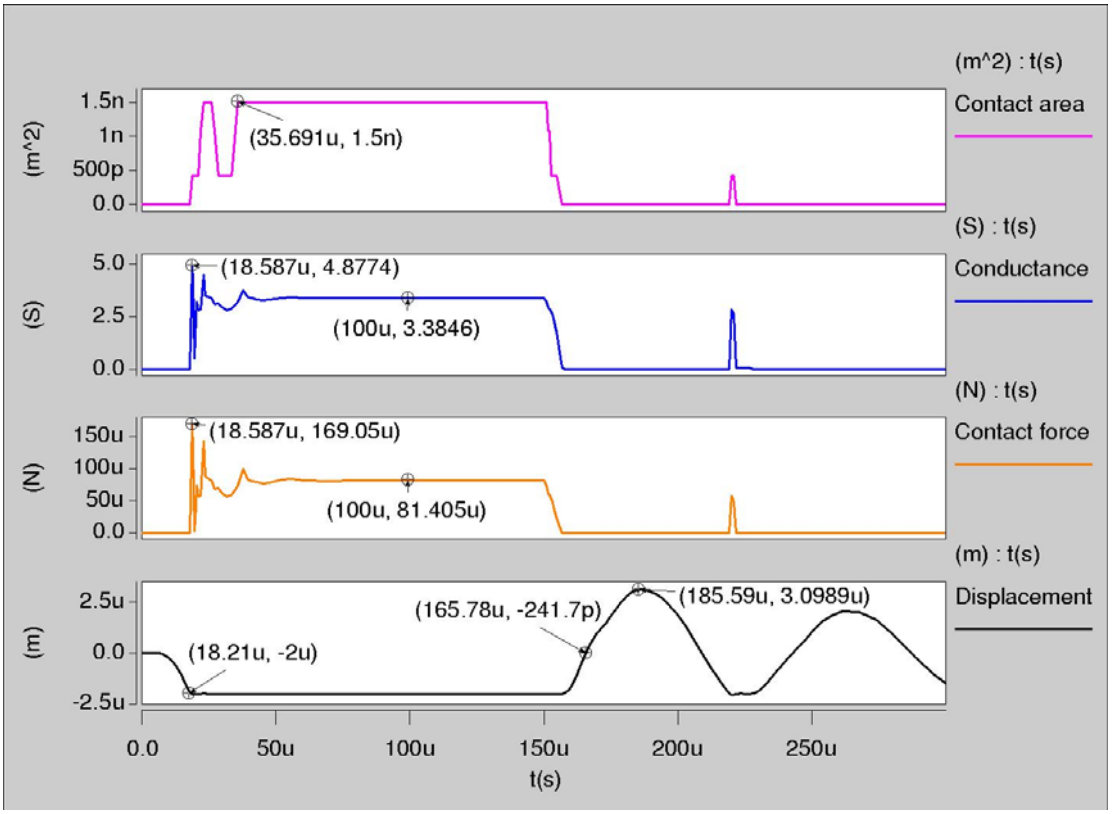

Fig. 11. Flowchart of the required steps for applying the Hybrid control mode

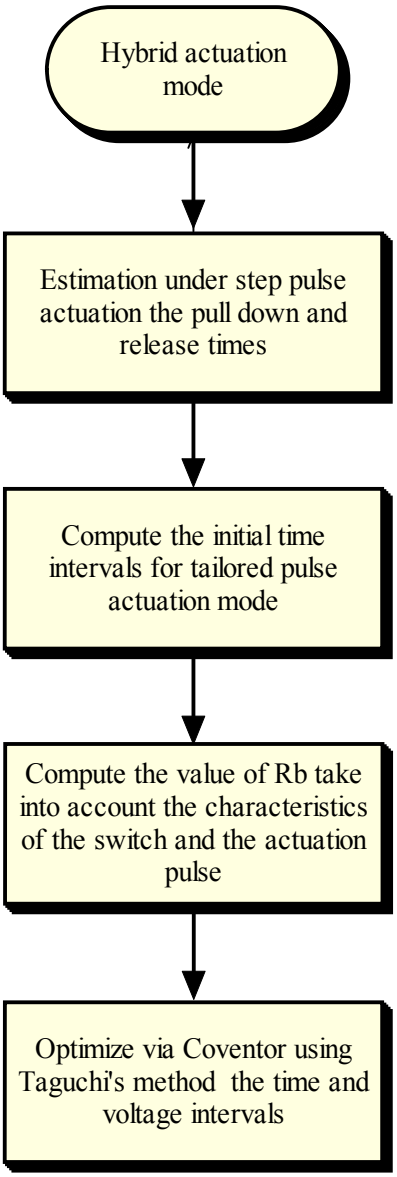

Fig. 12. Characteristics of the Hammerhead switch under Hybrid control mode

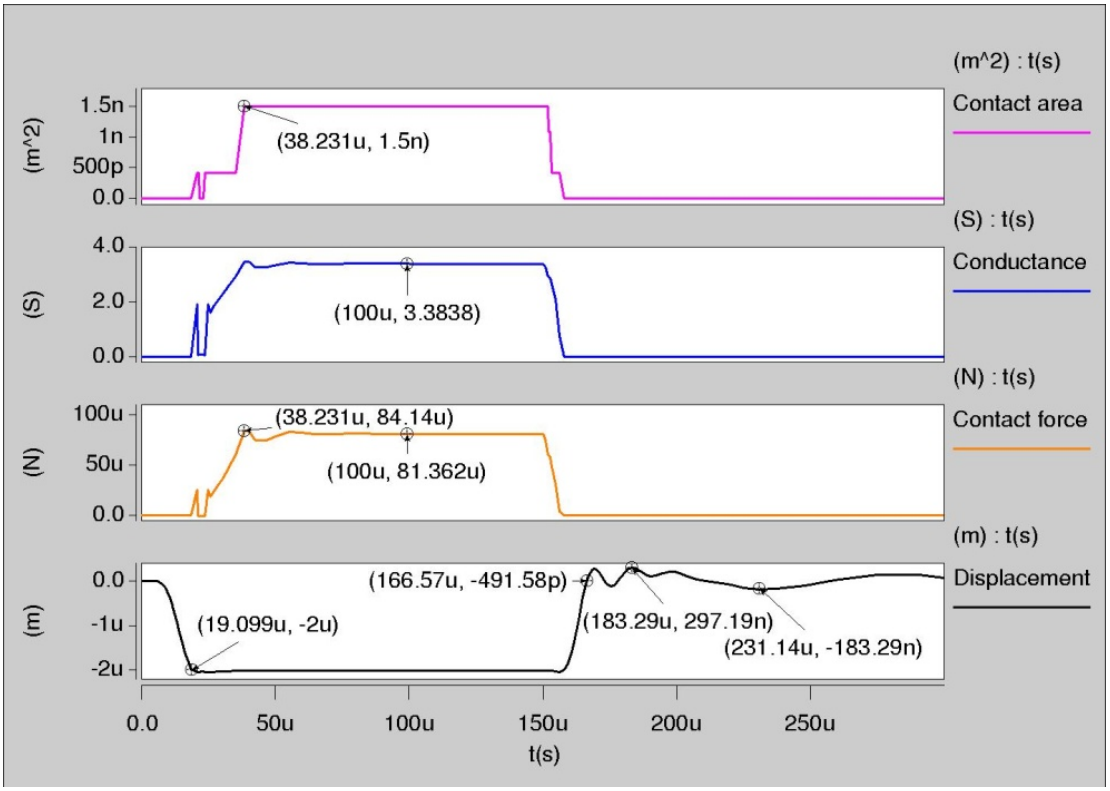

Fig. 13. Comparison between different actuation modes

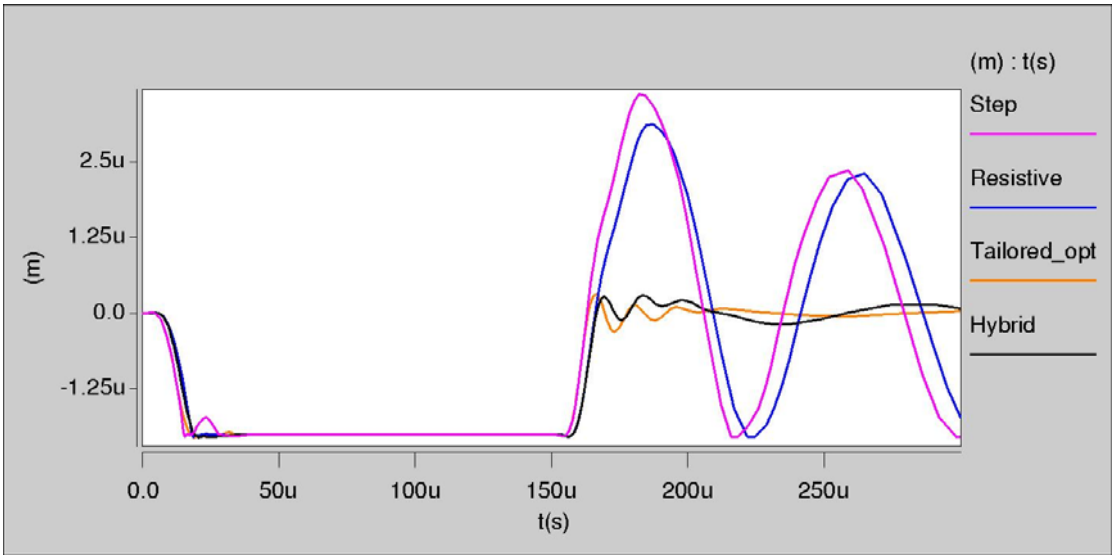

Fig. 14. Comparison between different actuation modes as concerns the pull-down phase

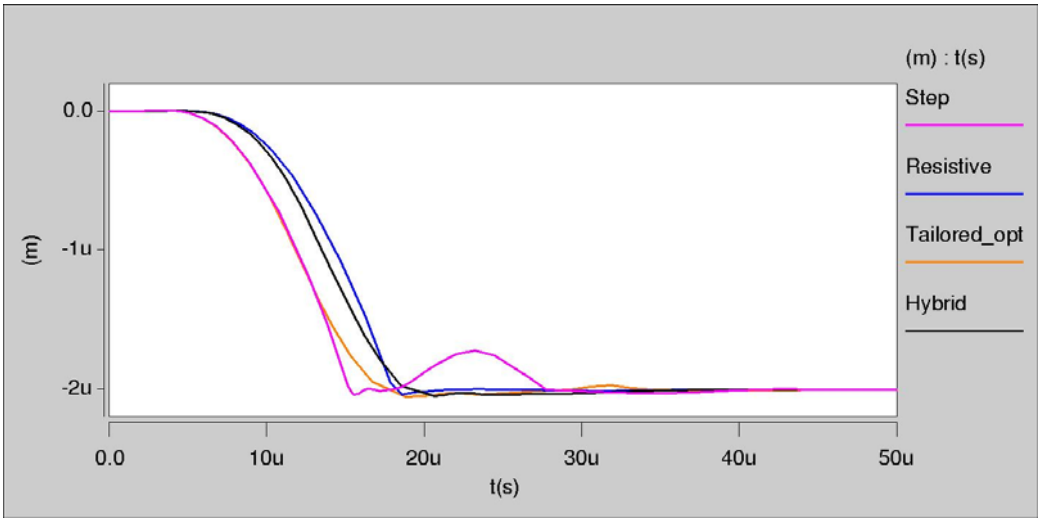

Fig. 15. Comparison of the contact forces

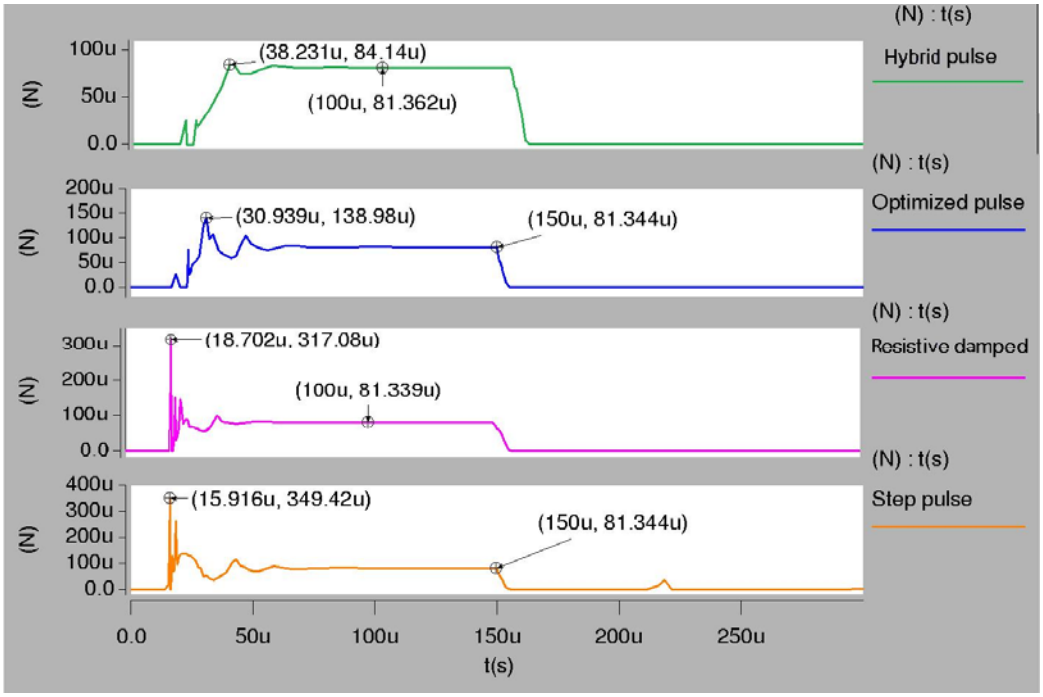

Fig. 16. Displacement and contact force figures of 2nd case under Hybrid mode

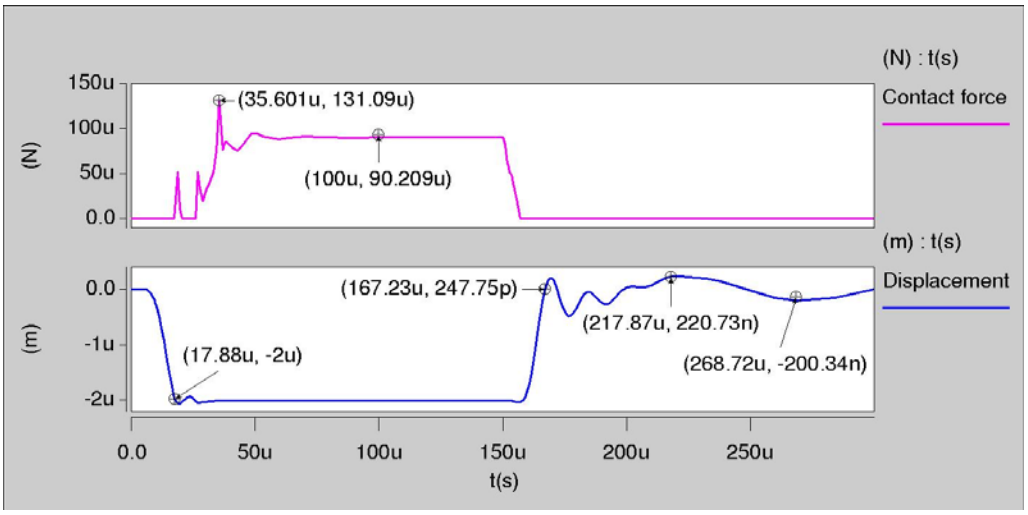

Fig. 17. Displacement and contact force figures of 4nd case under Hybrid mode

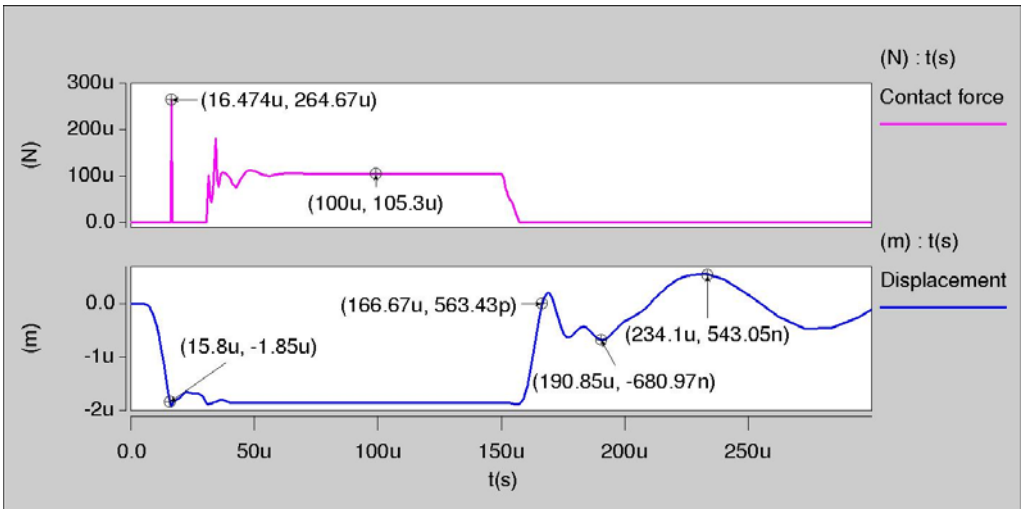

Table captions:

Table 1: Design parameters of the "Hammerhead" switch

Parameter	Value	Parameter	Value
Length (movable)	330μm	Contact force	81.3μN
Width	150μm 210μm	Conductance (total)	6.76S
Height from electrode	3μm	Pull-in(V_{pi}) V Nominal (V_{nom})	25.234 60V
Height from contacts	2μm	Capacitance (OFF)	12.3fF 6.15fF/per contact area
Cantilever Type	Gold	Rayleigh gas damping parameters	α=16547/s β=0.351μs
Cantilever thickness	6μm	Q_{GAS}	3.865
Holes to cantilever	Yes	Contact Area	$2x1.5nm^2$
Resonance frequency	12173Hz	Mesh type (Manhattan bricks)	5μm x 5μm x 6μm

Table 2. Pull-down phase (t_p) levels

	Pull-down phase (t_p) levels		
Vp (Volts)	48	60	72
$t_{p(on)}$ (μsec)	5.6	7	8.4
t_f (μsec)	1.6	2	2.4
$t_{p(off)}$ (μsec)	8.8	11	13.2
t_r (μsec)	1.6	2	2.4

Table 3. Release phase (t_r) levels

	Release phase (t_f) levels		
Vp (Volts)	48	60	72
$t_{r(on)}$ (μsec)	3.2	4	4.8
t_r (μsec)	1.6	2	2.4
$t_{r(off)}$ (μsec)	6.4	8	9.6
t_r (μsec)	1.6	2	2.4

Table 4. $OA_{18}(3^5)$

n rows	A	B	C	D	E
1	1	1	1	1	1
2	2	2	2	2	2
3	3	3	3	3	3
4	1	1	2	2	3
5	2	2	3	3	1
6	3	3	1	1	2
7	1	2	1	3	2
8	2	3	2	1	3
9	3	1	3	2	1
10	1	3	3	2	2
11	2	1	1	3	3
12	3	2	2	1	1
13	1	2	3	1	3
14	2	3	1	2	1
15	3	1	2	3	2
16	1	3	2	3	1
17	2	1	3	1	2
18	3	2	1	2	3

Table 5. Voltage and time intervals of the optimized tailored pulse

Pull-down phase (t_p)					**Release phase (t_r)**				
V_{p-d}	t_{p-on}	t_{p-f}	t_{p-off}	t_{p-r}	V_r	t_{r-off}	t_{r-r}	t_{r-on}	t_{r-f}
61.5V	7.3μs	1.6μs	10.2μs	2.2μs	61.5V	4.9μs	1.9μs	9.3μs	1.9μs

Table 6. Step pulse voltage and time values

t(μs)	0	2	150	152
V(V)	0	60	60	0

Table 7. Tailored pulse voltage and time values

t(μs)	0	2	9	11	22	24	150	152	156	158	166	168
V(V)	0	60	60	0	0	60	60	0	0	60	60	0

Table 8. Optimized tailored pulse voltage and time values

t(μs)	0	2	9.3	10.9	21.1	23.3	150	152	156.9	158.8	168.1	170.
V(V)	0	61.5	61.5	0	0	60	60	0	0	61.5	61.5	0

Table 9. Comparison of switching characteristics

	Impact Velocity	**Impact Force**	**Switching (pull down)**	**Switching (release)**	**Max. Bouncing Displacement**
Step Pulse	31cm/s	349μN	15.3μs	13.2μs	3.59μm, -2μm
Tailored Pulse	5.1cm/s	174μN	18.5μs	14.9μs	0.37μm, -0.33μm
Optimized-Tailored Pulse	3.6cm/s	138μN	17μs	13.7μs	0.11μm, -0.09μm

Table 10. Voltage and time intervals (Hybrid mode)

Pull-down phase (t_p)					**Release phase (t_r)**				
V_{p-d}	**t_{p-on}**	**t_{p-f}**	**t_{p-off}**	**t_{p-r}**	**V_r**	**t_{r-off}**	**t_{r-r}**	**t_{r-on}**	**t_{r-f}**
66V	7.5µs	1.9µs	9.7µs	1.9µs	61V	6.5µs	2.2µs	8.6µs	2.2µs

Table 11. Optimized tailored pulse voltage and time values (Hybrid mode)

t(µs)	0	2	9.5	11.4	21.1	23	150	152	158.5	160.7	169.3	171.5.
V(V)	0	66	66	0	0	60	60	0	0	61	61	0

Table 12. Comparison of switching characteristics

Mode	**Impact Velocity**	**Impact Force**	**Switching (pull-down)**	**Switching (release)**	**Max. Bouncing Displacement**
Step Pulse	31cm/s	349µN	15.3µs	13.2µs	3.59µm - 2µm
Optimized-Tailored Pulse	3.6cm/s	138µN	17µs	13.7µs	0.11µm - 0.09µm
Resistive damped	9.4cm/s	317µN	18.2µs	15.78µs	3µm - 2 µm
Hybrid	1.4cm/s	84µN	19µs	16.57µs	0.18µm - 0.18 µm

Table 13. The four parameters in three levels assigned in a $OA_9 3^4$ (Hammerhead)

n rows	Thickness (µm)	Height (µm)	Young modulus (MP)	Voltage (V)
1	5.7	2.75	78	57
2	5.7	3	57	60
3	5.7	3.15	99	63
4	6	2.75	57	63
5	6	3	99	57
6	6	3.15	78	60
7	6.3	2.75	99	60
8	6.3	3	78	63
9	6.3	3.15	57	57

Table 14. Results under optimized tailored pulse actuation mode implementation

Cases	t_s (µs)	F_{impact} (µN)	Bounce (Y/N)	$F_{contact}$ (µN)	Release swing (µm)	Failure (Y/N)
1	16.4	125.3	N	51.1	±0.38	N
2	-	-	-		-	Y
3	24.7	114.1	N	52.1	±0.88	N
4	-	-	-	-	-	Y
5	28.3	181.9	N	37.2	±0.78	N
6	26.3	165.9	N	46.8	±1.1	N
7	23.7	82.8	N	45.2	±0.78	N
8	20.2	85.1	N	55.4	±0.91	N
9	27.2	200.4	N	41.6	±1.21	N

Table 15. Results under "Hybrid" actuation mode implementation

Cases	**t_s (μs)**	**F_{impact} (μN)**	**Bounce (Y/N)**	**$F_{contact}$ (μN)**	**Release swing (μm)**	**Failure (Y/N)**
1	19.6	53.4	N	46.1	±0.35	N
2	17.8	131.1	Y	90.2	±0.22	N
3	25.1	58.7	N	51.3	±0.2	N
4	15.8	264.6	Y	105.3	±0.54	N
5	31.3	100.7	N	37	±0.2	N
6	27.9	83.4	N	46.4	±0.21	N
7	22.3	52.1	N	45.1	±0.09	N
8	20.8	63.3	N	56.2	±0.25	N
9	29	81.7	N	44.6	±0.53	N